

Three-dimensional diagnosis of pavement damage using CT scanner

S. Taniguchi & I. Nishizaki

Public Works Research Institute, Tsukuba, Japan

A. Moriyoshi

Emeritus Professor, Hokkaido University, Sapporo, Japan

ABSTRACT: Recently, the quality of pavement has been evaluated by examining the surface deformation and deflection either visually, or by an automated pavement surface measuring device. However, these methods evaluate only the pavement surface or estimate the quality of each layer. In this study, we developed a technique for three-dimensionally diagnosing the cause and degree of pavement damage. A 3-D crack analysis of each sample was conducted using a CT scanner and a 3-D void analysis program. 3-D images of in-situ specimens showed that longitudinal cracking occurred from not the surface or bottom but within pavement. The technique can thus be used to directly identify the 3-D pavement damage of each layer; it can easily and precisely diagnosis the position and level of damage in asphalt concrete pavement.

1 INTRODUCTION

Recently, the quality of pavement has been evaluated by examining the surface deformation and deflection either visually, or by an automated pavement surface measuring device, namely a falling weight deflectometer (FWD). However, these evaluation methods are one- or two-dimensional, and cannot evaluate the damage within pavement, since the qualities of each layer are evaluated or estimated from the surface of pavement. As a result, the deflection measured by FWD may be exactly the same in two sections on a expressway, even though one section has suffered longitudinal cracking but the other has not. These surface evaluation methods cannot easily detect damage under the binder course, yet such damage may cause longitudinal cracking on the surface. These phenomena and the required repair thickness cannot be grasped by evaluating the surface only. Furthermore, it is extremely difficult to diagnose the present conditions and residual service period of a pavement structure including the binder course or under-course.

We have therefore developed a new technology to three-dimensionally diagnose the repair time and depth of pavement structure. 3-D images of cracks are obtained by a micro-focus CT scanner (CT) and 3-D void analysis program, and are used to diagnose the structure within the pavement.

2 CRACKING OF ASPHALT CONCRETE PAVEMENT

2.1 Type of Cracking

Many countries have reported similar types of pavement cracking. For example, the Distress Identification Manual (Miller 2003) based on Long Term Pavement Performance (LTPP) in the Strategic Highway Research Program (SHRP) lists methods for surveying six types of cracking (fatigue cracking, block cracking, edge cracking, longitudinal cracking, reflection cracking at joints, and transverse cracking) in asphalt concrete pavement.

The causes of most of these types of cracking are known. For example, fatigue cracking is caused by insufficient pavement thickness or deterioration of bearing capacity on the aggregate base course or subgrade, reflection cracking is caused by joints or cracking on concrete slabs (Taniguchi 1998), and transverse cracking is caused by thermal stress. However, the fundamental cause of longitudinal cracking on the surface is not well understood, except for cracking mainly in the pavement on longitudinal ribs of orthotropic steel decks bridge. Since this phenomenon was reported, research on longitudinal cracking has made little progress. The next section describes longitudinal cracking in detail.

2.2 Longitudinal Cracking

In Japan, there has been severe flow rutting caused by heavy vehicles and the adoption of the “lane principle” since around 1970. Consequently, polymer modified asphalt (PMA) to reduce wear (PMA-I) and flow rutting (PMA-II) has been developed and standardized in the Manual for Asphalt Pavement (Japan Road Association 1989). In addition, high viscosity PMA (PMA-H), which has higher adhesive strength between aggregate and asphalt than existing asphalt, has spread since the Tokyo Metropolitan Government first constructed porous asphalt concrete pavement (PACP), which drains rain water and reduces noise, in 1987. Figure 1 shows the shipment of PMA in Japan as of 2000.

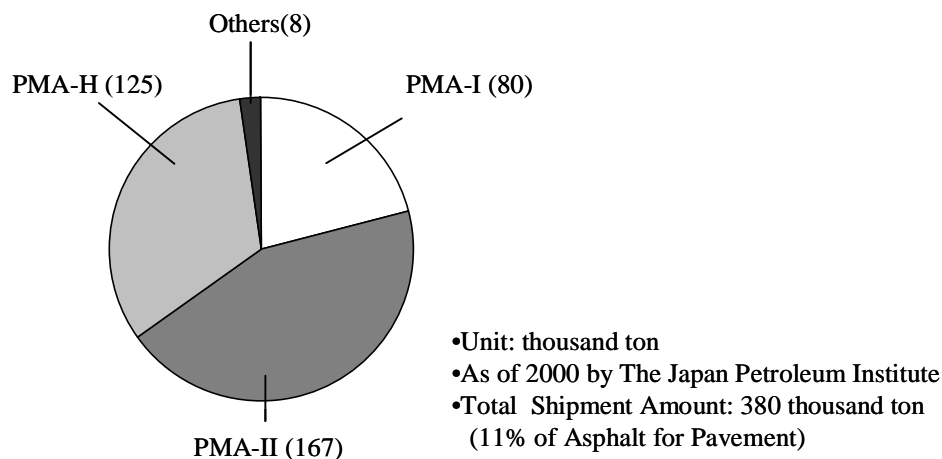


Figure 1. Shipment of modified asphalt in Japan

However, longitudinal cracks have been found as PMA has spread (Molenaar 1984 and Matsuno 1984). This type of cracking is usually called “top-down cracking” (Washington University and Freitas 2003, etc.) because core samples show that the crack is wider at the surface than at the bottom of pavement. Even if the crack reaches the bottom of pavement, it has been confirmed by viscoelastic simulation analysis that the crack is wider at the surface than at the bottom. Longitudinal cracking is also called “*Wadachiware*” because the cracks occur near the wheel path. Such cracking has occurred all over Japan (Komoriya 2001).

Indoor TRRL-type wheel tracking tests have shown that a large strain of 10% or more (which exceeds the maximum strain of the mixture of 1% at high speed and high temperature) is generated between aggregates even in the binder course (Abd-Alla 2006). It was also reported that longitudinal cracking occurred at not only the wheel path (outer wheel path, OWP) but also

the non wheel path (between wheel paths, BWP) in the LTPP GPS-6 and SPS-5 section (Federal Highway Administration 2000a, 2000b).

The causes of these pavement structure phenomena must be investigated not only at the surface layer and places where cracking occurs, but also below the binder course and places where cracking does not occur.

3 EXISTING EVALUATION METHODS

This section describes the automated pavement surface measuring device and FWD, and discusses the problems of these devices regarding pavement evaluation.

3.1 *Automated Pavement Surface Measuring Device*

Figure 2 shows a road surface measuring vehicle. It uses non-contact measurement by CCD camera or laser beam, and easily and automatically measures cracks, longitudinal profile and transverse profile under high speed traffic condition. The vehicle can safely and quickly measure the condition of the road surface without traffic lane closures. The automated pavement surface measuring device is also part of the pavement management system (PMS). The length of national highway administered by the Ministry of Land, Infrastructure, Transportation and Tourism (MLIT) is about 22,000 km, of which it surveys about 7,300 km each year. Thus, these vehicles cover all national highways every 3 years. Candidate sections for repair and the construction method are mainly decided considering rutting depth.



Figure 2. Automated pavement surface measuring device

3.2 *FWD*

The falling weight deflectometer (FWD) has been developed and researched since 1960 to evaluate the structure and damage of pavement based on dynamic deflections (Bohn 1972). FWD was introduced in 1983 and 30 units for measuring road pavement are in use as of February 2008 in Japan. Figure 3 shows the FWD held by the Public Works Research Institute (PWRI).

The estimation of elastic modulus from surface deflection measured by FWD has been widely studied and backcalculation programs have been developed to calculate the elastic modulus in each layer. FHWA published the Guideline for Review and Evaluation of Backcalculation Results (Stubstad 2006), and a back-calculation program called GAMES was developed in Japan (Maina 2004). Besides, “Evaluation Method for Pavement Performance” (Japan Road Association 2007) was published, and provides a graph for estimating acceptable number of wheel passes before fatigue failure of the pavement structure based on the initial deflection measured by FWD as shown in Figure 4.



Figure 3. FWD held by PWRI

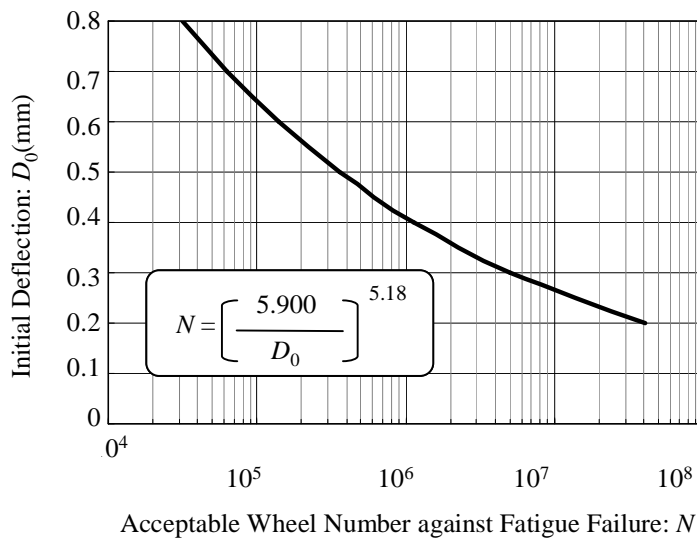


Figure 4. Relationship between acceptable number of wheel passes before fatigue failure and initial deflection

3.3 Problems of Crack Evaluation Method

Although the road surface measuring vehicle can measure the condition of the pavement surface, it cannot measure the quality inside the pavement structure. Furthermore, although FWD can estimate the elastic modulus in each layer, it cannot precisely and directly diagnose within the pavement structure and degree of damage in asphalt pavement is not evaluated by the elastic modulus.

Hence, to diagnose the pavement structure directly, this paper suggests a pavement diagnosis method based on images obtained by CT-scanning using cores sampled at a highway in service, and 3-D crack analysis.

4 OUTLINE OF THIS RESEARCH

4.1 Section

Specimens were collected in 2004 from two different sections on the same expressway (Section A and Section B), which were about 10 km apart and consisted of drainage pavement (surface course) with different asphalt properties (Taniguchi 2008). The sections are in a cold area in Japan, were put into service in 1999, and carry about 2,500 vehicles a day. Figure 5 shows the sections after five years of service. A visual examination shows almost no cracks or rutting on the surface of Section A, but a number of longitudinal cracks and slight rutting can be seen on Section B shown in Figure 5. In an ordinary pavement evaluation, the evaluation score was much higher for Section A than Section B.

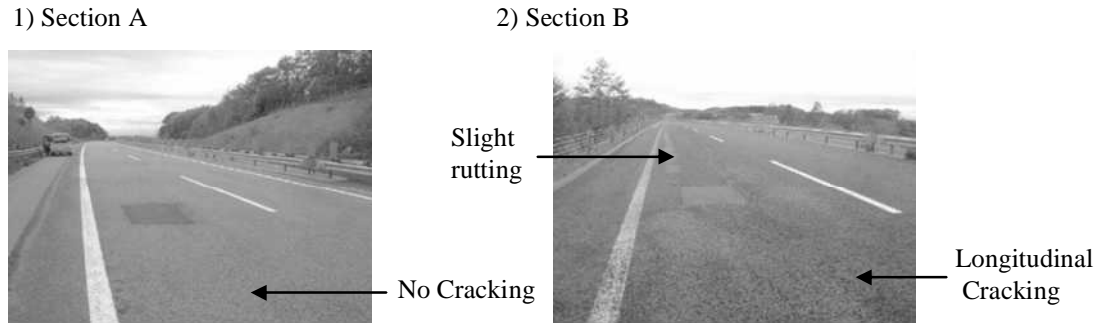


Figure 5. Surface condition of section A and section B

4.2 Condition of Materials and Construction

Figure 6 shows the compositions of the surface course, binder course and asphalt treated base in sections A and B. Porous asphalt concrete using PMA-H as binder was paved on the surface course in both sections. Table 1 shows the properties of PMA-H for sections A and B. The same straight asphalt (penetration grade: 60/80) was used for the binder course and asphalt treated base in both sections. Figure 7 shows the grain size distribution in both sections. Table 2 shows the binder content and Table 3 shows the compaction conditions of the asphalt pavement.

Rectangular samples, measuring 20 cm in width by 30 cm in length, were cut from the outer wheel path (OWP) and between wheel paths (BWP) at each section by a diamond cutter. These samples consisted of a layer of surface course, two layers of binder course, and two or three layers of asphalt treated base. Rectangular solid samples for CT-scanning measuring 2.5 cm in thickness, 2.5 cm in length and 10 cm in width were cut from these layers. Samples were cut small to evaluate the crack width and shape exactly. When large rectangular samples were collected, marks showing the direction of movement of vehicles were kept, and it was considered that the direction of samples cut small kept on turning to the direction of movement of vehicles.

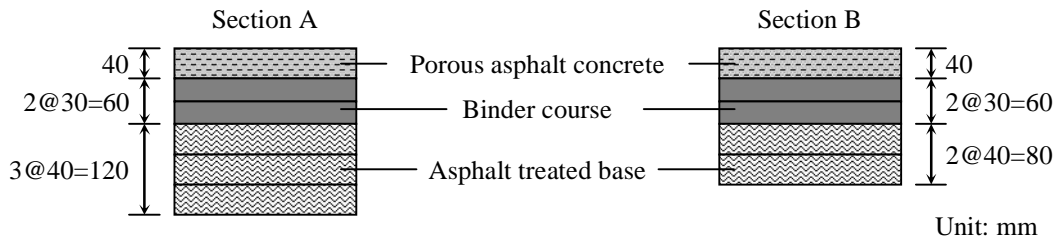


Figure 6. Composition of surface course, binder course and asphalt treated base

Table 1. Properties of PMA-H for sections A and B

	Section A		Section B	
	Recovered	Original	Recovered	Original
Penetration (25°C, 100 gr, 10 sec) [1/10 mm]	27	79	22	51
Softening point [°C]	93.0	98.5	94.0	95.0
Ductility (15°C) [cm]	24	100+	13	80
Density [g/cm ³]	1.043	1.020	1.051	1.025

Table 2. Binder content

	Surface	Binder	As. base
Binder content	5.5%	5.2%	4.2%

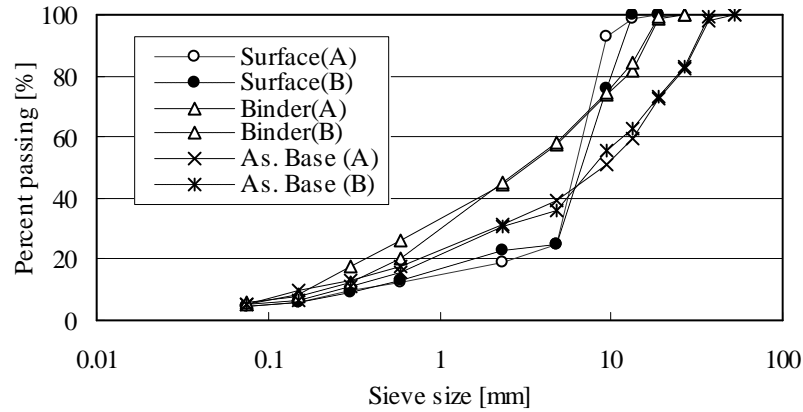


Figure 7. Grain size distribution

Table 3. Conditions of compaction in asphalt pavement

	Layer	Initial Compaction	Second Compaction	Finish Compaction
Section A	Surface	Macadam	Macadam	Tire Roller
		Roller	Roller	15t (8 times)
		12t (6 times)	12t (6 times)	80°C or lower
	Binder	Macadam	Tire Roller	Tire Roller
		Roller	25t (8 times)	25t (4 times)
		12t (4 times)	120±10°C	100°C or higher
	As. Base	Macadam	Tire Roller	Tire Roller
		Roller	25t (4 times)	15t (8 times)
		12t (4 times)	120±10°C	110°C or higher
Section B	Surface	Macadam	Macadam	Tire Roller
		Roller	Roller	15t (8 times)
		12t (10 times)	12t (10 times)	80°C or lower
	Binder	Macadam	Tire Roller	Tire Roller
		Roller	15t (4 times)	25t (10 times)
		12t (4 times)	120±10°C	90°C or higher
	As. Base	Macadam	Tire Roller	Tire Roller
		Roller	15t (4 times)	25t (6 times)
		12t (4 times)	120±10°C	90±10°C

4.3 CT-scanning and 3-D Analysis

Figure 8 shows a flow chart of the CT-scanning and special 3-D void analysis. Table 4 shows the specifications of CT (JRC JAZ-1300). Volume rendering (VG Studio MAX 2000) and void data processing (ExFact Analysis for porous/particles 2.0) were used in this analysis.

CT scanning was carried out as follows. As the turntable table on which a sample is placed makes one revolution, the sample is subjected to a cone-beam type X-ray for 3 minutes and the detector receives the X-ray through the sample. A computer records information for each degree of rotation of the X-ray collected by the detector. This information is data for the X, Y, and Z directions for the whole of each volume divided into 512^3 . From this information, firstly the inside of the sample is arranged in every volume of 0.24 mm^3 units, then the existence of aggregates and voids, etc. is arranged with a computer, and finally the data is reconfigured and a 3-D shape is rearranged.

The special 3-D void analysis software collates the X-ray gray scale information of the whole volume every 0.24 mm , and separates this small object inside aggregate, void, etc. The information provided by this software clearly shows the position, shape, and thickness of the crack in the sample.

Analysis images usually can be shown in three dimensions and using a 7-color scale. The size of the crack is clearly visible since it is shaded blue for large cracks and red for small cracks. In the gray scale, the brightness is dark for large cracks and light for small cracks.

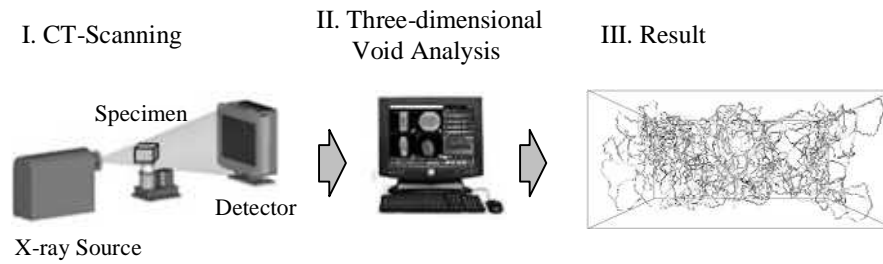


Figure 8. Flow chart of CT-scanning and special 3-D void analysis

Table 4. Specifications of CT-scanner

X-Ray: Minimum focus size:	8 μm
X-Ray: Maximum voltage:	130 kV
X-Ray: Maximum current:	300 μA
X-Ray: Maximum power:	39 W
Maximum load capacity of platform:	1 kg
Pixel area:	19.5 x 24.4 cm
Size of receiver:	26.67 x 31.75 cm
Size of micro-focus CT scanner:	W132 x H140 x D94 (cm)

4.4 Results of 3-D Analysis

Figure 9 shows the 3-D cracking distribution from the transverse side in the surface course, binder course and asphalt treated base under OWP and BWP at both sections A and B. In addition, Figure 10 shows the 3-D cracking distribution from the top, longitudinal and transverse sides in only the upper binder course at section A since remarkable longitudinal cracking was observed.

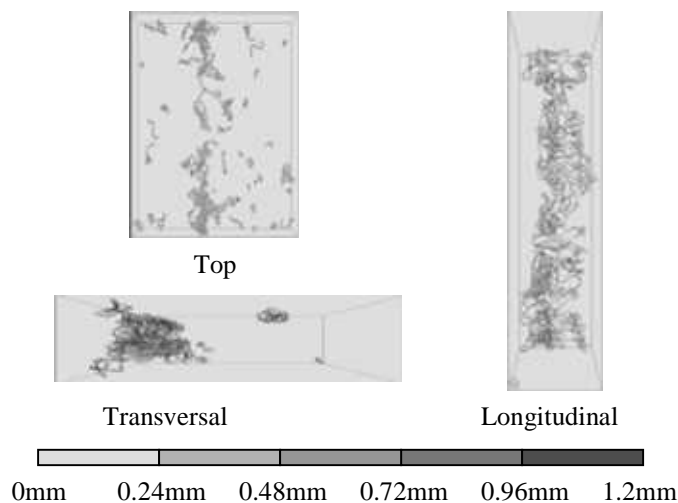
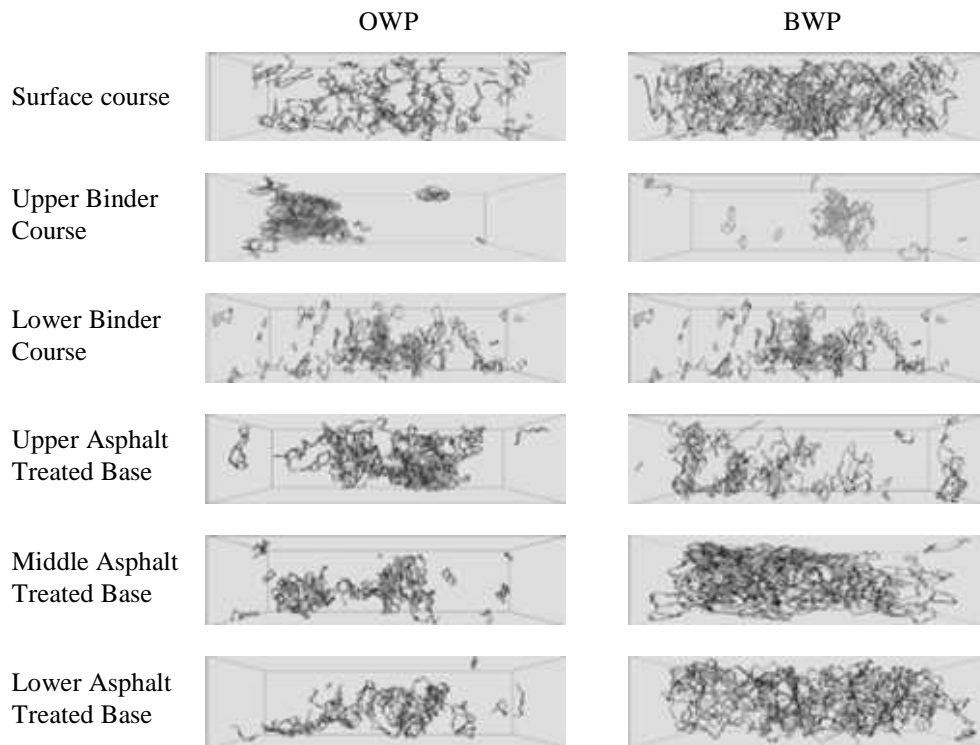


Figure 10. 3-D cracking distribution side in upper binder course at section A

1) Section A



2) Section B

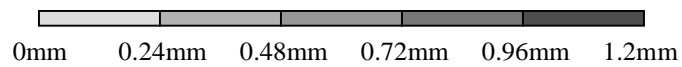
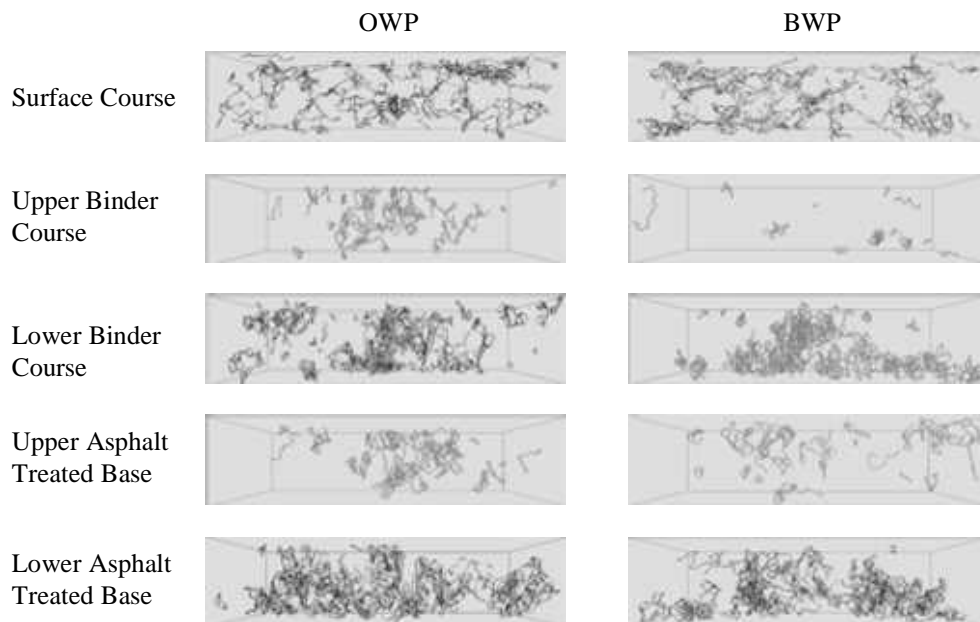


Figure 9. 3-D void distribution (Transverse side)

5 DISCUSSION

As shown in Figure 9, there was almost no cracking and rutting in the surface at section A. However, the three images in Figure 10 show that longitudinal cracking occurred in the upper binder course under OWP at section A. In addition, the longitudinal cracking observed at section B probably originated from the lower binder course since cracking is large in the lower binder course under BWP. Consequently, longitudinal cracking on asphalt concrete pavement occurs not only from the surface but also from within the asphalt concrete. Therefore, it is necessary to survey the inner part of the asphalt concrete layer, as it is impossible to specify the cause of longitudinal cracking from cutting and observing cores.

In addition, large cracking is revealed by 3-D images in the binder course and asphalt treated base under BWP at both sections. This indicates that longitudinal cracking occurs in not only the wheel path but also the non wheel path sections. This appears to be longitudinal cracking in the non wheel path at LTPP GPS-6 and SPS-5.

Thus, 3-D pavement diagnosis is possible using CT-scanning images and 3-D void analysis software. The images enable the place and degree of cracking on asphalt concrete pavement to be diagnosed easily and precisely. It is also possible to decide the optimum milling overlay thickness and reduce the life-cycle cost by determining the degree of damage in the asphalt concrete pavement structure.

6 CONCLUSIONS

This study revealed the following regarding longitudinal cracking on asphalt concrete pavement:

- Longitudinal cracking on asphalt pavement occurs from not only the pavement surface but also the inside.
- Cracking of pavement using PMA is observed in not only the wheel path but also the non wheel path sections.
- Cracking is observed in the layer under the binder course at both sections, and this damage is not always the largest in the wheel path.

The following results about pavement evaluation were also obtained.

- The type of pavement distress and degree of damage within the pavement structure cannot be obtained by means such as core observation, automated pavement surface measuring devices, and FWD.
- 3-D images analyzed by CT-scanner and the 3-D void analysis program help to diagnose the inside of the pavement structure easily and precisely.

The mechanism of damage in asphalt concrete pavement using PMA can be determined by using this diagnosis method and identifying the crack situation in not only the wheel path but also the non wheel path sections.

REFERENCES

- Abd-Alla E. M., Moriyoshi A., Part 1, M. N., Takahashi K., Kondo T. and Tomoto T., 2006. New Wheel Tracking Test to Analyze Movements of Aggregates in Multi-layered Asphalt Specimens, J. Jpn. Petrol. Inst., Vol. 49, No. 5
- Bohn A., Vllidtz P., Strubstad R. and Sorensen A., 1972. Danish Experiments with the French Falling Deflectometer, 3rd International Conference on the Structural Design of Asphalt Pavements, Vol. 1, p. 1119
- Federal Highway Agency, 2000a. Performance Trends of Rehabilitated AC Pavements, FHWA Tech Brief, FHWA-RD-00-165
- Federal Highway Agency, 2000b. Comparison of Rehabilitation Strategies for AC Pavements, FHWA Tech Brief, FHWA-RD-00-166
- Freitas E. and Pereira P. 2003. Assessment of Top-Down Cracking Cause in Asphalt Pavements, Proc. of 3rd International Symposium of Maintenance and Rehabilitation of Pavements and Technological

Control

- Japan Road Association, 1988. Manual for Asphalt Pavement
- Japan Road Association, 2007. Evaluation Method for Pavement Performance (in Japanese)
- Komoriya K., Yoshida T. and Nitta H.: "WA-DA-CHI-WA-RE" Surface Longitudinal Cracks on Asphalt Concrete Pavement, Transportation Research Board 80th Annual Meeting, CD-ROM Proceedings, January 2001
- Maina J. W. and Matsui K., 2004. Development of Software for Elastic Analysis of Pavement Structure due to Vertical and Horizontal Surface Loadings, Journal of Transportation Research Board, No. 1886, TRB, National Research Council
- Matsuno S. and Nishizawa T., 1984. Longitudinal Surface Cracking of Flexible Pavement, Proc. of Paving in Cold Area Mini-Workshop Canada/Japan Science and Technology Consultations, pp. 779-786
- Miller, J. S. and Bellinger Y., 2003. Distress Identification Manual for the Long-Term Pavement Performance Program, FHWA-RD-03-031, pp.1-13
- Molenaar A. A. A., 1984. Fatigue and Reflection Cracking Due to Traffic Roads, Proc. Ass. of Asphalt Paving Technologies, Vol. 54, pp. 454-496
- Stubstad R. N., Jiang Y. J. and Lukanen E. O. 2006. Guideline for Review and Evaluation of Backcalculation Results, FHWA-HRT-05-152
- Taniguchi S. and Ikeda T., 1998. Study in Reflective Cracking on Composite Pavement, Proc. of 5th International Conference on the Bearing Capacity of Composite Pavement
- Taniguchi S., Nishizaki I. and Moriyoshi A. 2008. A Study on Longitudinal Cracking in Asphalt Pavement Using CT Scanner, Road Materials and Pavements Design, Vol. 9/3, pp. 549-558
- Washington University. Pavement Guide Interactive, <http://training.ce.washington.edu/PGI/>